

## Calculation of the Second EXAFS Cumulant of Si Using the Anharmonic Correlated Einstein Model

Tran Thi Huyen Giang<sup>1</sup>, Do Ngoc Bich<sup>2</sup>, Vu Thi Kim Lien<sup>3</sup>

<sup>1,2,3</sup>Faculty of Fundamental Sciences, University of Fire Prevention and Fighting, Hanoi 120602, Vietnam

**ABSTRACT:** The second expanded X-ray absorption fine structure (EXAFS) cumulant of the crystalline silicon (Si) has been studied in the temperature-dependent. This is calculated in explicit forms using the anharmonic correlated Einstein (ACE) model developed from the correlated Einstein model based on the anharmonic effective potential and the quantum statistical theory. The numerical results of Si in the temperature range from 0 to 1200 K are in good agreement with those obtained by the other theoretical models and experiments at several temperatures. The analytical results show that the ACE model is suitable for analyzing the experimental EXAFS data of diamond cubics.

**KEYWORDS:** second EXAFS cumulant, ACE model, thermal disorders, crystalline silicon

### I. INTRODUCTION

Nowadays, the expanded X-ray absorption fine structure (EXAFS) has been widely used to determine many thermodynamic properties and structural parameters of materials, so it has been developed into a powerful technique [1]. However, thermal vibration disorders lead to the anharmonic effect of EXAFS oscillation and will smear out the EXAFS signals [2], as seen in Figure 1.

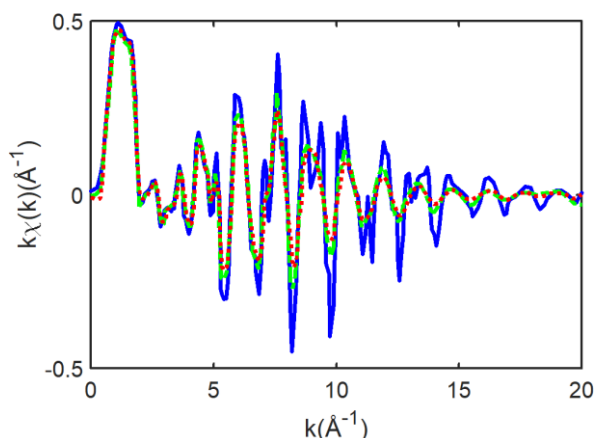


**Figure 1. The anharmonic EXAFS signals were extracted from the experiments [3].**

The *K*-edge XAFS signal includes a non-Gaussian disorder for a given scattering path is expressed in terms of a canonical average of all distance-dependent factors by [4]

$$\chi(k, T) = \frac{N e^{-2k^2 \sigma^2(T)} f(k)}{k R^2(T)} \sin[2kR(T) + \delta(k)] \quad (1)$$

where  $k$  is the wave number of the photoelectron,  $f(k)$  and  $\delta(k)$  characterizes scattering parameters of the photoelectron,  $\sigma^2(T)$  is the second EXAFS cumulant,  $R(T)$  is the distance to the neighboring atom, and  $N$  is the number of neighboring atoms.

In the investigation of the anharmonic EXAFS signal, the second EXAFS cumulant  $\sigma^2(T)$  is an important parameter [5]. It is because this cumulant is the mean-square relative displacement (MSRD) that describes the thermal disorder in the neighbor distance and determines the anharmonic EXAFS amplitude reduction via factor  $\exp\{-2k^2 \sigma^2(T)\}$  [6], as seen in Eq. (1).

Currently, crystalline silicon (Si) is the most important semiconductor in the electronics and technology sectors, and it includes solar cells, transistors, high-power lasers, semiconductors, rectifiers, and other solid-state devices [7]. Meanwhile, the experiment measured the second EXAFS cumulants of Si at 80 K, 300 K, and 500 K, measured at the Synchrotron Radiation Center by Benfatto *et al.* [8].

Recently, an anharmonic correlated Einstein (ACE) model has been applied to effectively treat the anharmonic EXAFS cumulant of crystals [9]. This model has the advantage that the obtained expressions are explicit and valid both in the low-temperature (LT) and high-temperature (HT) regions [10]. Hence, the calculation of the second EXAFS cumulant of Si using the ACE model will be a necessary addition to the experimental EXAFS analysis technique.

## II. FORMALISM AND CALCULATION MODEL

In the anharmonic EXAFS theory, the second cumulant can be explicitly related to low-order moments of true RD function, which can be determined as follows [11]:

$$\sigma^2(T) = \left\langle (r - \langle r \rangle)^2 \right\rangle = \left\langle (x - \langle x \rangle)^2 \right\rangle = \langle x^2 \rangle - \langle x \rangle^2, \quad (2)$$

where the angular bracket  $\langle \rangle$  is the thermal average,  $x$  is the deviation distance between the backscattering and absorbing atoms, and  $r$  is the instantaneous bond length between atoms.

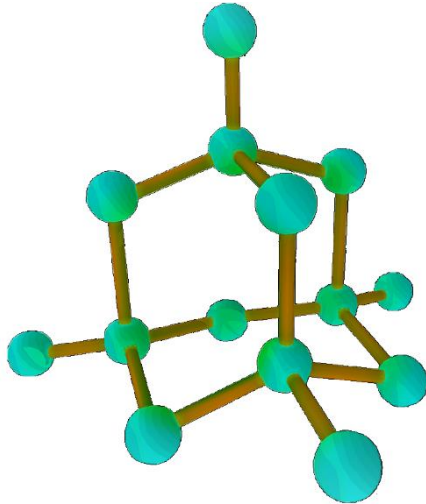


Figure 2. The structural model of Si.

The structural model of c-Si is illustrated in Figure 2. It can be seen that atoms are arranged with eight atoms in a diamond-cubic unit cell [12]. In this structure, all atoms are similar, and each atom is bonded covalently with four other surrounding atoms in the first shell [13].

Usually, the Morse potential can validly determine the pair interaction (PI) potential of the crystals [14]. If this potential is expanded up to the three orders around its minimum position, it can be written as

$$\varphi(x) = D \left( e^{-2\alpha x} - 2e^{-\alpha x} \right) \cong -D + D\alpha^2 x^2 - D\alpha^3 x^3 + \frac{7}{12} D\alpha^4 x^4, \quad x = r - r_0 \quad (3)$$

where  $D$  is the dissociation energy,  $\alpha$  is the width of the potential, and  $r_0$  is the equilibrium bond length between atoms.

Usually, an anharmonic effective (AE) potential can specify the thermodynamic parameters of crystals [13]. This potential can be determined from the PI potential of atoms. The AE potential can be calculated from the PI potential [10]:

$$V_{eff} = \varphi(x) + \sum_{i=A,B} \sum_{j \neq A,B} \varphi(\varepsilon_i x \hat{R}_{AB} \hat{R}_{ij}), \quad \varepsilon_i = \frac{\mu}{M_i}, \quad x = r - r_0 \quad (4)$$

where  $\mu = M_A M_B / (M_A + M_B)$  is the reduced mass of the backscatterer with masse  $M_A$  and absorber with masse  $M_B$ , sum  $i$  is the over backscatter ( $i = A$ ) and absorber ( $i = B$ ), the sum  $j$  is over the nearest neighbors,  $\hat{R}$  is a unit vector.

Using the Morse potential in Eq. (3) to calculate the AE potential according to Eq. (4) and ignoring the overall constant, we obtain the result as

$$V_{eff}(x) = V(x) + 3V\left(-\frac{1}{6}x\right) + 3V\left(\frac{1}{6}x\right) \square \frac{1}{2}k_{eff}x^2 - k_3x^3 + k_4x^4, \quad (5)$$

where  $k_{eff}$  is the effective force constant, and  $k_3$  and  $k_4$  are anharmonic force constants.

The local force constants are calculated from Eq. (5) and deduced as follows:

$$k_{eff} = \frac{7}{3} D\alpha^2, \quad k_3 = \frac{35}{36} D\alpha^3, \quad k_4 = \frac{1519}{2592} D\alpha^3, \quad (6)$$

The ACE model was developed from the CE model based on the first-order perturbation (FOP) theory and AE potential [10]. In this model, the atomic thermal vibrations in the crystal lattice of Si can be characterized by the correlated Einstein temperature  $\theta_E$  and frequency  $\omega_E$  [14]. These parameters can be defined as follows:

$$\omega_E = \sqrt{\frac{k_{eff}}{\mu}} = \alpha \sqrt{\frac{14D}{3m}}, \quad \theta_E = \frac{\hbar\omega_E}{k_B} = \frac{\hbar\alpha}{k_B} \sqrt{\frac{14D}{3m}}, \quad (7)$$

where  $\hbar$  and  $k_B$  are the reduced Planck and Boltzmann constants, respectively.

Usually, the second EXAFS cumulants can be presented in terms of the power moments  $\langle x^k \rangle$  with  $\langle \rangle$  is the thermal average and are approximated via the statistical density matrix within the quantum-statistical theory [15]. The general expressions of the temperature-dependent EXAFS cumulants in the ACE model were calculated by Hung *et al.* [10].

Substituting the expressions of effective force constants  $k_{eff}$  in Eq. (6) into the general expression of the second EXAFS cumulant, we obtain the temperature-dependent second XAFS cumulant in the form as

$$\sigma^2(T) = \frac{3\hbar\omega_E}{14D\alpha^2} \left( \frac{e^{\hbar\omega_E/k_B T} + 1}{e^{\hbar\omega_E/k_B T} - 1} \right). \quad (8)$$

Using an approximation,  $\exp\{\hbar\omega_E/k_B T\} \approx 1 + \hbar\omega_E/k_B T$ , we calculate the second EXAFS cumulant of Si in the LT limit ( $T \rightarrow 0$ ) from Eq. (8). The obtained result is

$$\sigma^2(T) = \frac{\sqrt{42\hbar}}{14\alpha\sqrt{mD}}. \quad (9)$$

Using the approximation  $\exp\{\hbar\omega_E/k_B T\} \approx 0$ , we calculate the second EXAFS cumulant of Si in the HT limit ( $T \rightarrow +\infty$ ) from Eq. (8). The obtained result is

$$\sigma^2(T) = \frac{3k_B T}{7D\alpha^2}. \quad (10)$$

Thus, the ACE model has been extended to efficiently calculate the second EXAFS cumulat of Si. The expressions obtained using this model can satisfy all their fundamental properties in temperature dependence.

### III. RESULTS AND DISCUSSION

In this section, the numerical results of  $W$  are calculated using the ACE model based on the obtained expressions in Secs. 2 and their physical parameters, which are the atomic mass  $m = 28.09$  u [16] and Morse potential parameters  $D = 1.83$  eV,  $\alpha = 1.56$  Å<sup>-1</sup>, and  $r_0 = 2.34$  Å [17]. We calculate using Eqs. (6) and (7) in the ACE model and obtain the local force constants  $k_{eff} \square 10.39$  eVÅ<sup>-2</sup>,  $k_{an} \square 6.75$  eVÅ<sup>-3</sup>, the correlated Einstein frequency  $\omega_E \square 8.42 \times 10^{13}$  Hz, and the correlated Einstein temperature  $\theta_E \square 643.49$  K.

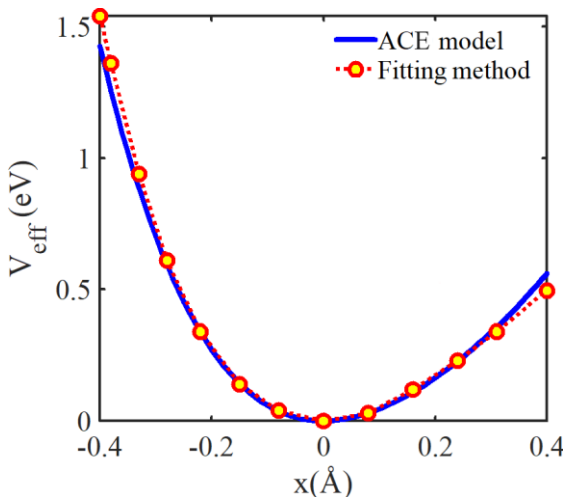


**Figure 3. The position-dependent AE potential of Si is obtained from the ACE model and fitting method [19].**

The position dependence of the AE potential of Si in the position range from - 0.4 to 0.4 Å is represented in Figure 3. Our obtained result using the ACE model is calculated using Eqs. (5) and (6), while the fitting result is obtained from a reactive empirical bond-order potential of c-Si by fitting its bond-order terms [19]. Our result agrees better with those obtained from the fitting method [19], especially at positions far from the minimum position. Moreover, the influence of anharmonic effects on the AE potential is stronger at

positions further away from the minimum position of this potential. Moreover, the obtained result using the anharmonic correlated Debye (ACD) model [20] is similar to our result because this model also uses Eqs. (5) and (6) in calculations.

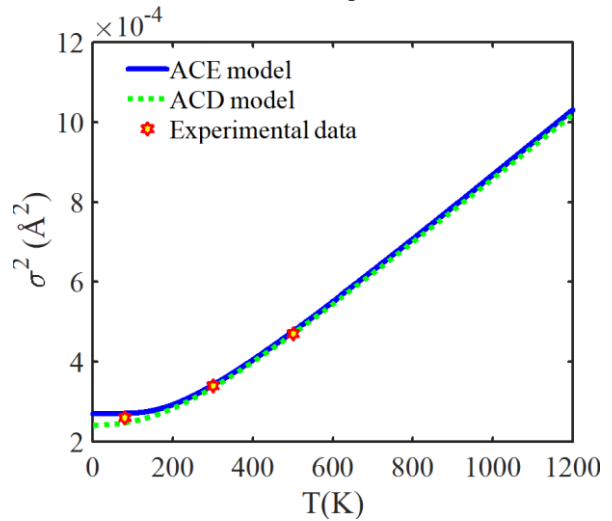


**Figure 4. Temperature-dependent second EXAFS cumulant of Si is obtained using the ACE and ACD [20] models and experimental data [8].**

The temperature dependence of the second EXAFS cumulant  $\sigma^2(T)$  of Si in a range from 0 K to 1200 K is represented in Figure 4. Our obtained result using the ACE model is calculated by Eq. (8). It can be seen that our results are in agreement with those obtained using the ACD model [20] and experimental data [8]. For example, the obtained results using the ACE model, ACD model, and experimental data at  $T = 300$  K are  $\sigma^2 \square 4.42 \times 10^{-4}$  Å<sup>2</sup>,  $\sigma^2 \square 4.36 \times 10^{-4}$  Å<sup>2</sup> [20], and  $\sigma^2 \square 4.40 \times 10^{-4}$  Å<sup>2</sup> [8], respectively. Moreover, it can be seen that the ACE and ACD [20] models both show quantum effect contributions, but the obtained results using the ACE model in the LT region are slightly greater. This can be explained by the ACE model using only one effective frequency to describe the atomic thermal vibrations, as seen in Figure 4.

Thus, the calculated results of the second EXAFS cumulant using the present ACE model satisfied all of their fundamental properties in temperature dependence. This obtained result shows that the second EXAFS cumulant decreases with increasing temperature  $T$  and can also describe the anharmonic effect in the HT region and the quantum effect in the LT region.

### IV. CONCLUSION

In this work, we have successfully applied the ACE model to calculate the second EXAFS cumulant of Si. The temperature-dependent expression can satisfy all of their fundamental properties and can express the EXAFS amplitude increasing strongly with temperature  $T$ . These results can also describe the influence of the anharmonic effect at high temperatures and the influence of the quantum

effect at low temperatures on the EXAFS signal. The good agreement between our numerical results of Si and those obtained using the ACD model and experimental data at various temperatures shows the effectiveness of the present model. This model can be applied to analyze the experimental EXAFS data of diamond cubics from above absolute zero temperature to just before the melting point.

#### ACKNOWLEDGMENTS

The author would like to thank Assoc. Prof. T.S. Tien for their helpful comments. This work was supported by the University of Fire Prevention and Fighting, Hanoi 120602, Vietnam.

#### REFERENCES

1. P. Fornasini, R. Grisenti, M. Dapiaggi, G. Agostini, and T. Miyanaga, Nearest-neighbour distribution of distances in crystals from extended X-ray absorption fine structure, *Journal of Chemical Physics* 147(4) (2017) 044503.
2. R.B. Gregor and F.W. Lytle, Extended x-ray absorption fine structure determination of thermal disorder in Cu: Comparison of theory and experiment, *Physical Review B* 20(12) (1979) 4902-4907.
3. G. Dalba, P. Fornasini, and M. Grazioli, Local disorder in crystalline and amorphous germanium, *Physical Review B* 52(15) (1995) 11034-11043.
4. M. Newville, Fundamentals of XAFS, *Reviews in Mineralogy & Geochemistry* 78(1) (2014) 33-74.
5. P. Fornasini and R. Grisenti, On EXAFS Debye-Waller factor and recent advances, *Journal of Synchrotron Radiation* 22 (2015) 1242-1257.
6. P. Eisenberger and G.S. Brown, The study of disordered systems by EXAFS: Limitations, *Solid State Communications* 29(6) (1979) 481-484.
7. M.G. Voronkov, Silicon era, *Russian Journal of Applied Chemistry* 80(12) (2007) 2190-2196.
8. M. Benfatto, C.R. Natoli, and A. Filipponi, Thermal and structural damping of the multiple-scattering contributions to the x-ray-absorption coefficient, *Physical Review B* 40(14) (1991) 9626-9635.
9. T.S. Tien, N.V. Nghia, C.S. Thang, N.C. Toan, and NB Trung, Analysis of temperature-dependent EXAFS Debye-Waller factor of semiconductors with diamond crystal structure, *Solid State Communications* 352 (2022) 114842.
10. N.V. Hung and J.J. Rehr, Anharmonic correlated Einstein-model Debye-Waller factors, *Physical Review B* 56(1) (1997) 43-46.
11. T. Fujikawa and T. Miyanaga, Quantum Statistical Approach to Debye-Waller Factors in EXAFS, EELS and ARXPS. I. Anharmonic Contribution in Plane-Wave Approximation, *Journal of the Physical Society of Japan* 62(11) (1993) 4108-4122.
12. C. Kittel, *Introduction to Solid State Physics*, Eighth ed., John Wiley & Sons, New York, 2004.
13. S.H. Simon, *The Oxford Solid State Basics*, First ed., Oxford University Press, Oxford, 2013.
14. L.A. Girifalco and V.G. Weizer, Application of the Morse Potential Function to Cubic Metals, *Physical Review* 114(3) (1959) 687-690.
15. T. Yokoyama, K. Kobayashi, T. Ohta, and A. Ugawa, Anharmonic interatomic potentials of diatomic and linear triatomic molecules studied by extended x-ray-absorption fine structure, *Physical Review B* 53 (1996) 6111-6122.
16. N.V. Hung, T.S. Tien, N.B. Duc, and D.Q. Vuong, High-order expanded XAFS Debye-Waller factors of HCP crystals based on classical anharmonic correlated Einstein model, *Modern Physics Letters B* 28(21) (2014) 1450174.
17. P. Chalon, *Organic Chemistry: A Mechanistic Approach*, First ed., CRC Press, Boca Raton, 2015.
18. R.A. Swalin, Theoretical calculations of the enthalpies and entropies of diffusion and vacancy formation in semiconductors, *Journal of Physics and Chemistry of Solids* 18(4) (1961) 290-296.
19. J.D. Schall, G. Gao, and J.A. Harrison, Elastic constants of silicon materials calculated as a function of temperature using a parametrization of the second-generation reactive empirical bond-order potential, *Physical Review B* 77 (2008) 115209.
20. Tong Sy Tien, Application of Anharmonic Correlated Debye Model in Investigating Anharmonic XAFS Thermodynamic Properties of Crystalline Silicon, *VNU Journal of Science* 38(4) (2022) 25-35.